

Liquid State based Transfer Learning for 360 Image Transmission in Wireless Virtual Reality Networks

Mingzhe Chen*, Walid Saad†, and Changchuan Yin*

*Beijing Key Laboratory of Network System Architecture and Convergence,

Beijing University of Posts and Telecommunications, Beijing, China 100876, Emails: chenmingzhe@bupt.edu.cn, ccyin@ieee.org.

†Wireless@VT, Bradley Department of Electrical and Computer Engineering, Virginia Tech, Blacksburg, VA, USA, Email: walids@vt.edu.

Abstract—In this paper, the problem of 360° image transmission is studied for a wireless network of virtual reality (VR) users that communicate with cellular base stations (BSs). The VR users will send their uplink tracking information to the BS and receive the VR images in the downlink. To satisfy VR users' delay target, the BSs can change the image transmission format for each image requested by users so as to reduce the downlink traffic load. Meanwhile, the VR users can directly rotate the already received VR image and use the rotated VR images at a later time to further reduce the downlink traffic load. This 360° image transmission and image rotation problem is then formulated as an optimization problem whose goal is to maximize the users' successful transmission probability which is defined as the probability that the delay of tracking information and image transmission for each VR user satisfies the VR delay requirement. A liquid state machine (LSM) based transfer learning algorithm is proposed to solve this optimization problem. The proposed LSM-based transfer learning algorithm enables each BS to transfer the already learned successful transmission to the new successful transmission that must be learned so as to increase the convergence speed. Simulation results show that the proposed algorithm achieves 14.9% gain in terms of successful transmission probability compared to Q-learning.

I. INTRODUCTION

Virtual reality (VR) services are one of the most important applications of tomorrow's wireless 5G networks [1]. By leveraging wireless communications, a whole new range of VR applications can be developed. However, the data size of each 360° VR image will exceed 50 Mbits and the transmission delay requirement of each VR image must be less than 20 ms. In consequence, these VR requirements exceed the capacity of wireless cellular networks. One promising approach to meet the high data rate and low delay requirements of VR services is to transform the standard 360° VR images into cubic, pyramidal, or visible images [2] that have smaller data size compared to 360° images. To leverage such VR image transformations and effectively transmit VR data over wireless networks, many challenges need to be overcome [1], such as the extraction of cubic, pyramidal, and visible image, spectrum and computing resource allocation for VR users as well as the prediction of users' locations and orientations used for VR image extraction.

The existing literature has studied a number of problems related to VR image transmission in wireless VR systems such as in [3]–[7]. The authors in [3] developed a VR image transmission scheme that delivers only the visible portion of a 360° VR video based on the VR users' movement prediction. The work in [4] used a machine learning algorithm to guide a user's movement in a VR immersive application. However, the works in [3] and [4] focus on wired VR systems and do not consider any challenges of deploying VR systems over

wireless cellular networks. In [5], the authors implemented a WiFi experiment for a single wireless VR user. However, the work in [5] that uses WiFi connectivity to service only one wireless VR user within a single room may not be able to provide VR services for a network of outdoor VR users. In [6], the authors proposed a model for wireless VR networks and a machine learning approach for VR resource management. The work in [7] investigated the spectrum resource allocation problem with a brain-aware QoS constraint. However, most of these existing works in [3]–[7] do not consider the cubic, pyramidal, or visible image transmission which can significantly reduce the VR image data size that each base station (BS) needs to transmit so as to reduce the traffic load over BS-users links. Moreover, none of these existing works [3]–[7] consider the image rotation for VR image transmission. For instance, a VR image can be directly obtained by the rotation of a previously received VR image and, hence, the BSs will not need to transmit that VR image. For example, a given user changes its orientation and requests a new VR image. If the user received a 360° VR image before changing orientation, the user can directly rotate the 360° VR image without the VR image transmission from the BSs.

The main contribution of this paper is to propose a new transfer learning [8] approach for VR image transmission so as to maximize the users' successful transmission probability. *To our best knowledge, this is the first work that jointly considers the VR image transmission format with VR image rotation.* Our contributions of this work can be given as follows:

- We propose an image transmission method for wireless VR cellular networks using which BSs can transmit 360° standard, cubic, pyramidal, or visible images to the users. Meanwhile, the users can directly rotate an already received VR image to obtain a new VR image requested by users at a later time slot so as to reduce the traffic load over BS-users links. Therefore, the BSs must determine the image transmission format for each image that users request considering image rotation and VR delay requirement.
- We formulate this joint uplink tracking information transmission, downlink 360° image transmission, and image rotation problem as an optimization problem whose goal is to maximize the users' successful transmission probability.
- To solve this problem, we propose a liquid state machine (LSM) [9] based transfer learning algorithm to maximize the users' successful transmission probability. The proposed transfer learning algorithm can transform

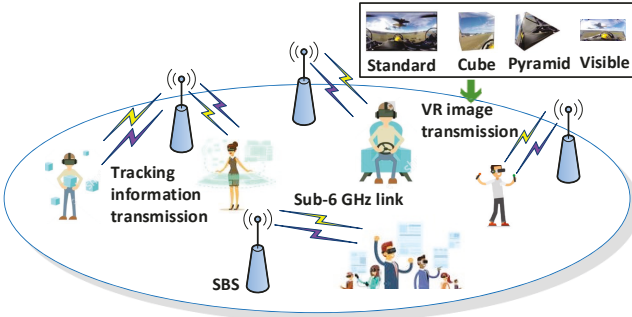


Fig. 1. A wireless VR network that consists of multiple BSs and VR users. In this model, the BSs can transmit various types of VR images to the users which, in turn, will transmit tracking informations to the BSs.

the already learned successful transmission into the new successful transmission that must be learned due to the change of users' image requests.

- Simulation results show that the proposed LSM-based learning algorithm can yield up to 14.9% gain of total successful transmission probability compared to Q-learning.

The rest of this paper is organized as follows. The system model and problem formulation are presented in Section II. The LSM-based transfer learning algorithm for image transmission is introduced in Section III. In Section IV, simulation results are presented and analyzed. Finally, Section V concludes the paper.

II. SYSTEM MODEL AND PROBLEM FORMULATION

Consider the downlink of a wireless cellular network that consists of a set \mathcal{B} of B BSs servicing a set \mathcal{U} of U wireless VR users. Each VR user will associate with its nearest BS. The BSs will transmit VR images to the users and the users will transmit the tracking information including users' locations and orientations to the BSs so as to generate the VR images requested by users, as shown in Fig. 1. We assume that all of the bandwidth of each BS will be allocated to its associated users.

A. VR Image Transmission Format

To enable the BSs to satisfy the VR users' delay target, we must reduce the data size of each VR image. The standard transmission format of a VR image is equirectangular [1]. To reduce the data size of a VR image, a VR image can be transformed from the standard equirectangular format into cubic, pyramidal, or visible formats as shown in Fig. 1. Using the cube, pyramid, or visible formats can reduce, respectively, 25%, 75%, and 90% of data size compared to using the standard format [2]. However, reducing the data size of a VR image will increase the number of VR images that need to be sent by the BS. This is due to the fact that as the data size of a VR image decreases, the number of the pixels used to construct a VR image decreases. In consequence, the users cannot rotate the VR image as their locations and orientations change. We use a set $\mathcal{C} = \{c_0, c_1, c_2, c_3\}$ to represent the formats of a VR image. Here, c_1 to c_4 , respectively, represent the standard, cube, pyramid, and visible transmission formats.

Based on the above formulation, the data size of each VR image a that user i requests is $S(f_{a_i})$ where $f_{a_i} \in \mathcal{C}$.

B. VR Image Transmission Model

In a VR network, the downlink is used to transmit VR images while the uplink is used to transmit users' tracking information. The data rate of VR image transmission from BS j to user i at time t can be given by:

$$c_{ji}^D(U_j(t)) = \frac{B^D}{U_j(t)} \log_2 \left(1 + \frac{P_B h_{ij}}{\sum_{n \in \mathcal{B}, n \neq j} P_B h_{in} + \sigma^2} \right), \quad (1)$$

where P_B is the transmit power of each BS j which is assumed to be equal for all BSs, h_{ij} is the channel gain between BS j and user i , and σ^2 is the variance of the Gaussian noise. B^D is the total bandwidth of each BS j used for VR image transmission. $U_j(t)$ is the number of users that request VR images at time t . Similarly, the data rate of tracking information transmission from user i to BS j at time t is:

$$c_{ji}^U(U_j(t)) = \frac{B^U}{U_j(t)} \log_2 \left(1 + \frac{P_U h_{ij}}{\sum_{n \in \mathcal{U}, n \neq i} P_U h_{nj} + \sigma^2} \right), \quad (2)$$

where P_U is the transmit power of each user i which is assumed to be equal for all users and B^U is the total bandwidth of BS j 's users used for tracking information transmission.

C. Transmission Delay Model

In the studied system, since VR images and tracking information are transmitted over downlink and uplink, respectively, the transmission delay over the uplink and downlink will directly affect the users' quality-of-experience. Next, we introduce the time used for VR image and tracking information transmission. In our model, a VR image that each user requests at time t can be obtained using one of two ways: a) the BS transmits the VR image to the user and b) the user can directly rotate the VR image that has been received at previous time. Let a_{it} be the VR image that user i requests at time t . We assume that a_{it}^R is the VR image that has been received before time slot t and $f_{a_{it}^R}$ is the image format of a_{it}^R . We also assume that each VR user can only store one VR image that has been received at nearest previous time slot. We can define $R(a_{it}, f_{a_{it}^R}) \in \{0, 1\}$ as the image rotation from VR image a_{it}^R to a_{it} . Here, $R(a_{it}, f_{a_{it}^R}) = 1$ indicates that image a_{it} can be obtained by the image rotation from image a_{it}^R , otherwise, $R(a_{it}, f_{a_{it}^R}) = 0$. Let A be the data size of each user's tracking information. For user i associated with BS j , the time used for VR image and tracking information transmission can be given by:

$$D_{ijt} \left(f_{a_{it}}, f_{a_{it}^R}, U_j(t), a_{it} \right) = \begin{cases} \frac{S(f_{a_{it}})}{c_{ij}^D(U_j(t))} + \frac{A}{c_{ij}^U(U_j(t))}, & R(a_{it}, f_{a_{it}^R}) = 0, \\ 0, & R(a_{it}, f_{a_{it}^R}) = 1, \end{cases} \quad (3)$$

where $\frac{S(f_{a_{it}})}{c_{ij}^D(U_j(t))}$ represents the time that BS j needs to transmit VR image a_{it} to user i and $\frac{A}{c_{ij}^U(U_j(t))}$ represents the time that user i needs to transmit tracking information to BS j . In (3), $R(a_{it}, f_{a_{it}}^R) = 1$ indicates that the VR image a_{it} that user i has requested at time t can be obtained by the rotation of the VR image a_{it}^R that user i received before time slot t . In consequence, BS j does not need to transmit VR image a_{it} to user i and, hence, the time used for VR image and tracking information transmission will be 0. (3) shows that the transmission delay depends not only on the number of users that request images from BS j , user i 's data rates, and transmission format $f_{a_{it}}$ but depends also on the transmission format $f_{a_{it}}^R$.

D. Problem Formulation

Given the defined system, we formulate an optimization problem whose goal is to maximize the successful transmission of users at each time t . This optimization problem is:

$$\max_{f_{a_{it}}} \sum_{j \in \mathcal{B}} \sum_{i \in \mathcal{U}_j} \frac{1}{T} \sum_{t=1}^T \mathbb{1}_{\{D_{ijt}(f_{a_{it}}, f_{a_{it}}^R, U_j(t), a_{it}) \leq \gamma_D\}}, \quad (4)$$

$$\text{s. t. } f_{a_{it}} \in \mathcal{C}, \quad \forall j \in \mathcal{B}, i \in \mathcal{U}_j, \quad (4a)$$

$$a_{it} \in \mathcal{N}, \quad \forall i \in \mathcal{U}_j, \quad (4b)$$

where γ_D is the maximum tolerable latency for each VR user (maximum supported by the VR system being used). \mathcal{N} is the set of all of contents that the VR users can request. (4a) indicates that each BS can transmit standard equirectangular, cube, pyramid, and visible images to the users. From (4), we can see that $\frac{1}{T} \sum_{t=1}^T \mathbb{1}_{\{D_{ijt}(f_{a_{it}}, f_{a_{it}}^R, U_j(t), a_{it}) \leq \gamma_D\}}$ is the successful transmission probability of each user i . Meanwhile, the image transmission format $f_{a_{it}}$ is discrete. Moreover, at each time slot t , the transmission delay of each user i depends not only on the image that user i requests at time t but also on the image a_i^R that user i received at previous time slot. In consequence, conventional optimization algorithms cannot be used to solve the problem in (4). Thus, a transfer learning [8] algorithm can be used to solve (4). This is due to the fact that the transfer learning algorithm can adaptively adjust the image transmission formats of each user as the users' image requests change. Moreover, the transfer learning algorithm can transform the already learned image transmission formats to the new image transmission formats that must be learned. For instance, a transfer learning algorithm can learn the change of the users' image requests between time slots t and $t+1$ and, hence, it can directly find the optimal image transmission format at time $t+1$ using the learned image transmission format at time t .

III. LIQUID STATE MACHINE BASED TRANSFER LEARNING FOR IMAGE TRANSMISSION

In this section, a transfer learning algorithm based on the machine learning framework of *liquid state machine* [10] is proposed. The proposed LSM-based transfer learning algorithm will equip each BS with the ability to select an

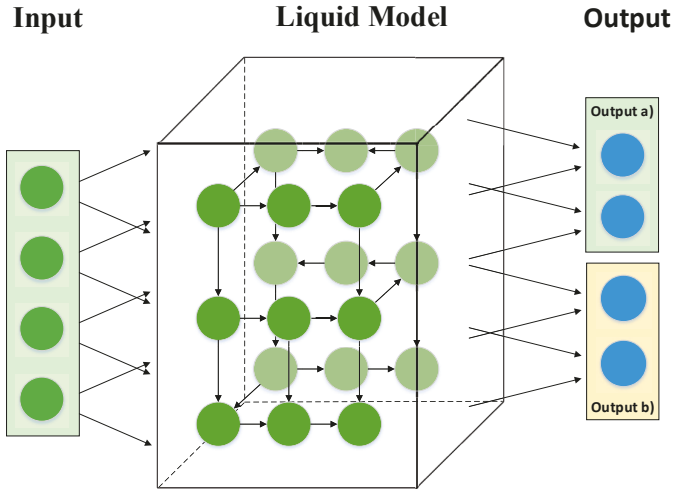


Fig. 2. The components of the LSM-based transfer learning approach.

appropriate image transmission format for each image that users request so as to maximize the successful transmission probability of each user. Moreover, the proposed LSM-based transfer learning algorithm can use the already learned information such as the actions that have been used and their corresponding value of successful transmission to directly learn the actions and the successful transmission values as the users' image requests change. In consequence, the proposed transfer learning algorithm can increase the convergence speed. Next, we first introduce the components of an LSM-based transfer learning algorithm. Then, we specify the entire procedure of each BS j using LSM-based transfer learning algorithm to solve the problem in (4).

A. Components of LSM-based Transfer Learning Algorithm

In the studied system, each BS j will implement one LSM-based algorithm that consists of four components: a) inputs, b) liquid model, c) actions, and d) output, as shown in Fig. 2. The components of the proposed LSM-based transfer learning algorithm are thus given as follows:

- **Input:** The LSM input is the users' image requests at time t , which is $\mathbf{a}_j(t) = [a_{1t}, \dots, a_{U_j^{\max} t}]^T$ where U_j^{\max} is the number of users associated with BS j .
- **Action:** The action of the LSM-based transfer learning algorithm is the image transmission format which can be given by $\mathbf{v}_j = [v_{1j}, v_{2j}, \dots, v_{U_j^{\max} j}]$ where $v_{ij} \in \{0, c_0, c_1, c_2, c_3\}$. Here, $v_{ij} = 0$ indicates that BS j will not send any images to user i at time t while $v_{ij} = c_0$, $v_{ij} = c_1$, $v_{ij} = c_2$, and $v_{ij} = c_3$, respectively, indicate that BS j will transmit standard, cube, pyramid, and visible images to user i . To improve the convergence speed of the proposed algorithm, action selection must be implemented based on the following rule:

Lemma 1. Given the image requests $\mathbf{a}_j(t)$ of the users associated with BS j , the image transmission format of user i can be given by:

- i) If $R(a_{it}, f_{a_{it}}^R) = 1$, $v_{ij} = 0$.

ii) If $R(a_{it}, f_{a_{it}^R}) = 0$ and $D_{ijt}(c_0, f_{a_{it}^R}, U_j^{\max}, a_{it}) \leq \gamma_D$, $v_{ij} = c_0$.

Proof. For i), the image that user i requests can be obtained by the rotation of the image that user i already received. In consequence, BS i has no need to transmit a VR image to user i . For ii), $v_{ij} = c_0$ indicates that BS j transmits the standard image to user i and $U_j(t) = U_j^{\max}$ indicates that all of the users associated with BS j request image at time t . In consequence, $D_{ijt}(c_0, f_{a_{it}^R}, U_j^{\max}, a_{it})$ is the maximum transmission delay for user i . $D_{ijt}(c_0, f_{a_{it}^R}, U_j^{\max}, a_{it}) \leq \gamma_D$ indicates that the delay of user i will always meet the delay requirement regardless of image transmission format. Therefore, if $D_{ijt}(c_0, f_{a_{it}^R}, U_j^{\max}, a_{it}) \leq \gamma_D$, BS j will transmit the standard image to user i so as to increase the probability that the image that user i will request at a later time slot can be obtained via the image rotation. This completes the proof. \square

From Lemma 1, we can see that the image transmission format at time t will affect the image transmission format at time $t+1$. This is due to the fact that at time t , if each BS transmits a large sized VR image, then the probability that user i can directly rotate this image and use it at time $t+1$ increases.

- *Output:* The LSM-based transfer learning algorithm has two outputs: a) predicted successful transmission probability and b) predicted deviation of the successful transmission as the users' image requests vary. The output a) of the proposed transfer learning algorithm can be used to build the relationship between the users' image requests a_j , actions v_j , and users' successful transmission probability $\sum_{i \in \mathcal{U}_j} \mathbb{P}_{it}$, where $\mathbb{P}_{it} =$

$\frac{1}{t} \sum_{n=1}^t \mathbb{1}_{\{D_{ijn}(f_{a_{in}}, f_{a_{in}^R}, U_j(n), a_{in}) \leq \gamma_D\}}$ is the successful transmission probability of user i at time t . Let $\mathbf{y}_j(t) = [y_{jv_{j1}}(t), \dots, y_{jv_{jN_{jv}}}(t)]^T$ be the output a) where $y_{jv_{jn}}(t)$ represents the predicted total successful transmission probability of BS j using action v_{jn} . N_{jv} represents the total number of actions of BS j .

The output b) is used to find the relationship between $\sum_{i \in \mathcal{U}_j} \mathbb{1}_{\{D_{ijt}(f_{a_{it}^R}, U_j(t), a_{it}) \leq \gamma_D\}}$ and $\sum_{i \in \mathcal{U}_j} \mathbb{1}_{\{D_{ijt+1}(f_{a_{it+1}^R}, U_j(t+1), a_{it+1}) \leq \gamma_D\}}$ as BS j only knows $\sum_{i \in \mathcal{U}_j} \mathbb{1}_{\{D_{ijt}(f_{a_{it}^R}, U_j(t), a_{it}) \leq \gamma_D\}}$. This implies that the proposed algorithm can transfer the value of total successful transmission that has been learned at time t to the new successful transmission that will be learned at time $t+1$. Therefore, we define the output b) of the proposed LSM-based transfer learning algorithm at time t as the predicted deviation of the total successful transmission when the users' image requests change. The output b) can be given by

$$\mathbf{y}'_j(t) = [y'_{jv_{j1}}(t), \dots, y'_{jv_{jN_{jv}}}(t)]^T \text{ where}$$

$$\begin{aligned} y'_{jv_{jk}}(t) = & \sum_{i \in \mathcal{U}_j} \mathbb{1}_{\{D_{ijt+1}(f_{a_{it+1}^R}, U_j(t+1), a_{it+1}) \leq \gamma_D\}} \\ & - \sum_{i \in \mathcal{U}_j} \mathbb{1}_{\{D_{ijt}(f_{a_{it}^R}, U_j(t), a_{it}) \leq \gamma_D\}}. \end{aligned}$$

- *LSM Model:* An LSM model that consists of a liquid model and output functions is used to find the relationship between the input $a_j(t)$ and the output $\mathbf{y}_j(t)$ as well as output $\mathbf{y}'_j(t)$. The liquid model consists of leaky integrate and fire neurons that are arranged in a three dimensional-column. The information state of each neuron n at time t can be given by $\varphi_{jn}(t)$ which can be given by [9]:

$$\varphi_{jn}(t) = \varphi_{jn}(t-1) + \frac{S + ZI_i(t-1) - \varphi_{jn}(t-1)}{Z\rho}, \quad (5)$$

where Z represents the neuron resistance, $I_i(t-1)$ is the input of neuron n , and ρ is a constant that captures the neuron state. Here, the probability that neurons i and j are connected with each other can be given by [9]:

$$P_{ij} = \varsigma e^{-(d(i,j)/\lambda)^2}, \quad (6)$$

where $\varsigma \in \{\varsigma_{\text{EE}}, \varsigma_{\text{EI}}, \varsigma_{\text{IE}}, \varsigma_{\text{II}}\}$ is a constant which depends on the type of neurons. In the studied liquid model, we consider two types of neurons: inhibitory neurons and excitatory neurons [9]. Here, ς_{EE} , ς_{EI} , ς_{IE} , and ς_{II} , respectively, represent an excitatory-excitatory connection, an excitatory-inhibitory connection, an inhibitory-excitatory connection, and an inhibitory-inhibitory connection.

The output function consists of two output weight matrices. We assume that each time slot t consists of $N_{\Delta t}$ time intervals and an LSM will record the information states of the neurons at each interval. Then, the output weight matrices can be given by $\mathbf{F}_j, \mathbf{F}'_j \in \mathbb{R}^{N_{jv} \times (N_w N_{\Delta t} + U_j^{\max})}$ where N_w is the number of the neurons in the liquid model.

B. LSM-based Transfer Learning for Image Transmission

At each time slot t , each BS j will receive the users' image requests and set the input $a_j(t)$ of the LSM-based transfer learning algorithm. Based on the input, the LSM will calculate the information states of the neurons located in the liquid model. The information states of the neurons during time t can be given by $\varphi_j(t) = [\varphi_j^1(t), \dots, \varphi_j^{N_{\Delta t}}(t)]$ where $\varphi_j^n(t) = [\varphi_{j1}^n(t), \dots, \varphi_{jN_w}^n(t)]$ represents the information states of all of the neurons at interval n and $\varphi_{jk}^n(t)$ is the information state of neuron k at interval n of time slot t . Based on the input $a_j(t)$ and the information states $\varphi_j(t)$ of neurons located in the liquid model, the LSM-based transfer learning algorithm will output the predicted successful transmission probability resulting from the actions of each BS, which is:

$$\mathbf{y}_j(t) = \mathbf{F}_j(t) \begin{bmatrix} \varphi_j(t) \\ a_j(t) \end{bmatrix}, \quad (7)$$

TABLE I
LSM-BASED TRANSFER LEARNING FOR IMAGE TRANSMISSION

```

for each time  $t$  do
    (a) Estimate the value of successful transmission probability
         $\sum_{i \in \mathcal{U}_j} \mathbb{P}_{it}$  based on (7).
    if  $t = 1$ 
        (b) Set the action selection policy uniformly.
    else
        (c) Set the action selection policy based on  $\epsilon$ -greedy [11].
    end if
    (e) Receive the users' image requests and set the input  $\mathbf{a}_j(t)$ .
    (f) Implement one action based on the  $\epsilon$ -greedy policy.
    (g) Calculate the actual successful transmission probability.
    (h) Calculate the information states of the neurons based on (5).
    (i) Update the output weight matrix  $\mathbf{F}_j$  according to (9).
    if  $t > 1$ 
        (j) Estimate deviation of successful transmission based on (8).
        (k) Calculate the actual deviation of the successful transmission.
        (l) Update the output weight matrix  $\mathbf{F}'_j$  according to (10).
    end if
end for

```

where $\mathbf{F}_j(t)$ is the output weight matrix a) at time t . Similarly, the LSM-based transfer learning algorithm will also need to learn the deviation of the successful transmission as the users' image requests vary at time t . Then, the output b) of the LSM-based transfer learning algorithm can be given by:

$$\mathbf{y}'_j(t) = \mathbf{F}'_j(t) \begin{bmatrix} \varphi_j(t) \\ \mathbf{a}_j(t) \end{bmatrix}, \quad (8)$$

where $\mathbf{F}'_j(t)$ is the output weight matrix b) at time t . To enable the LSM can predict the outputs a) and b), the output weight matrices $\mathbf{F}_j(t)$ and $\mathbf{F}'_j(t)$ must be updated as follows:

$$\mathbf{F}_{jn}(t+1) = \mathbf{F}_{jn}(t) + \delta \left(\sum_{i \in \mathcal{U}_j} \mathbb{P}_{it} - y_{j\mathbf{v}_{jn}}(t) \right) [\varphi_j(t) \mathbf{a}_j(t)], \quad (9)$$

and

$$\begin{aligned} \mathbf{F}'_{jn}(t+1) = & \mathbf{F}'_{jn}(t) + \delta' \sum_{i \in \mathcal{U}_j} \mathbb{1}_{\{D_{ijt}(\mathbf{v}_{jn}) \leq \gamma_D\}} [\varphi_j(t) \mathbf{a}_j(t)] \\ & - \delta' \left(\sum_{i \in \mathcal{U}_j} \mathbb{1}_{\{D_{ijt-1}(\mathbf{v}_{jn}) \leq \gamma_D\}} + y'_{j\mathbf{v}_{jn}}(t) \right) [\varphi_j(t) \mathbf{a}_j(t)], \end{aligned} \quad (10)$$

where $\mathbf{F}_{jn}(t+1)$ and $\mathbf{F}'_{jn}(t+1)$ represent the row n of output weight matrices $\mathbf{F}_j(t+1)$ and $\mathbf{F}'_j(t+1)$, respectively. δ and δ' are the learning rates. According to the above formulations, the distributed LSM-based transfer learning algorithm implemented by each BS j is summarized in Table I.

In this algorithm, the BSs can find the relationship between the image transmission strategy and its corresponding successful transmission probability. During each iteration, the LSM-based transfer learning algorithm will first record the actions that each BS takes and the corresponding successful transmission probability. Then, the LSM-based transfer learning algorithm can approximate the deviation of the successful transmission when the users' image requests change so as to increase the convergence speed. As time elapses, each BS j 's output resulting from action i will converge to two

TABLE II
SYSTEM PARAMETERS

Parameter	Value	Parameter	Value
B_D	1000	B_D	20 dBm
P_U	4	P_B	5, 5
N_w	100	σ^2	-105 dBm
T	1000	S	13.5 mV
Z	20 dB	ρ	30 ms
SEE	0.3	SEI	0.4
SE	0.2	SII	0.1
λ	2	$N_{\Delta t}$	10
δ	0.03	δ'	0.03

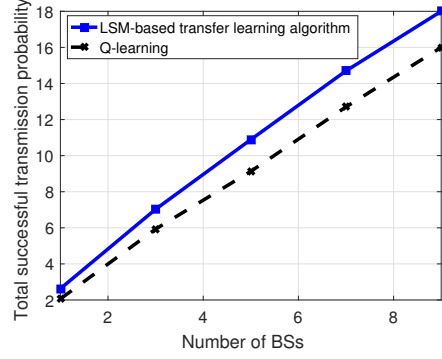


Fig. 3. Total successful transmission probability as the number of BSs changes.

final values $\sum_{i \in \mathcal{U}_j} \mathbb{P}_{it}$ and $\sum_{i \in \mathcal{U}_j} \mathbb{1}_{\{D_{ijt+1} \leq \gamma_D\}} - \sum_{i \in \mathcal{U}_j} \mathbb{1}_{\{D_{ijt} \leq \gamma_D\}}$. When the proposed LSM-based transfer learning algorithm converges, it can find the optimal image transmission policy for the VR users with different image requests.

IV. SIMULATION RESULTS

For our simulations, we consider a cellular network deployed in a circular area with radius $r = 500$ m. $U = 20$ users and $B = 4$ BSs are uniformly distributed in this area. The delay requirement γ_D of VR users will be 20 ms. The detailed parameters are listed in Table II. For comparison purposes, we use a baseline Q-learning algorithm in [11]. For this Q-learning algorithm, the input of Q-learning is the LSM's input \mathbf{a}_j , the actions of Q-learning are the actions defined in our LSM-based transfer learning algorithm, and the reward function $r(\mathbf{a}_j, \mathbf{v}_j)$ is the successful transmission probability \mathbb{P}_{it} .

In Fig. 3, we show how the total successful transmission probability changes as the number of BSs changes. From Fig. 3, we can see that, as the number of BSs increases, the total successful transmission probability increases. This is because, as the number of BSs increases, the users have more connection choices and the number of users associated with each BS decreases. Fig. 3 also shows that the proposed transfer learning algorithm can achieve up to 14.9% gain of total successful transmission probability compared to Q-learning for a network with 8 BSs. This gain stems from the fact that the proposed transfer learning algorithm has a larger memory capacity to record users' historical content requests, the actions that each BS uses, and their corresponding successful transmission compared to Q-learning that uses Q-table to record the historical informations. In consequence, the proposed algorithm can accurately predict the successful transmission probability of each BS.

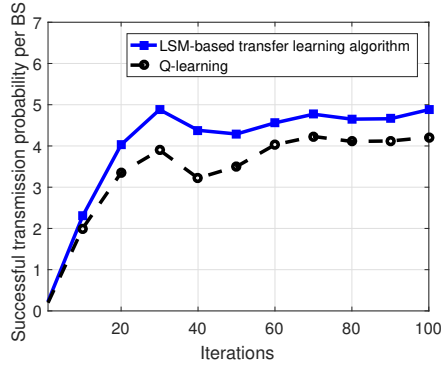


Fig. 4. Successful transmission probability of each BS as time elapses.

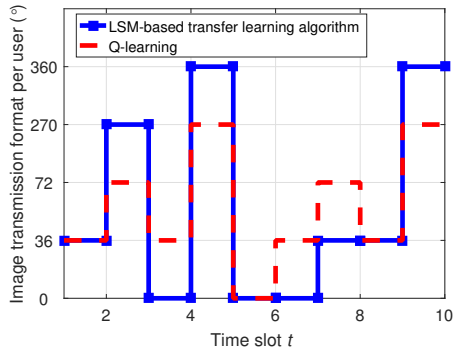


Fig. 5. Image transmission format of a given user as time elapses.

Fig. 4 shows how the successful transmission probability of each BS changes as time elapses. From Fig. 4, we can see that, each BS's successful transmission probability resulting from both the proposed algorithm and Q-learning changes as time elapses. This is due to the fact that as time elapses, the users' content requests change and, hence, the BS may not satisfy the delay requirement of each user at each time slot. Fig. 4 also shows that the deviation between the proposed transfer learning algorithm and Q-learning increases as time elapses. This is due to the fact that, as time elapses, the proposed transfer learning algorithm can transfer the already learned successful transmission to the new successful transmission that must be learned. However, as time continues to elapse, the deviation between the proposed algorithm and Q-learning remain a constant, this is because the training procedure of both the proposed transfer learning algorithm and Q-learning have finished and the gain stems from the prediction accuracy of the considered algorithms.

In Fig. 5, we show how the image transmission format of a given user changes as time elapses. In this figure, 36° , 72° , 270° , and 360° respectively, represent the visible, pyramid, cube, and standard image transmission format. 0 indicates that the user can directly rotate an already received VR image and, hence, the BS will not transmit any VR images to the user at that time slot. From Fig. 5, we can see that as time elapses, the BS transmits different format VR images to the user. This is due to the fact that, as time elapses, the number of users that request VR images varies. In consequence, the bandwidth allocated to each user will be changed. To satisfy the delay requirement, the BS needs to change the image transmission format for each user at each time slot. Fig. 5 also shows that, at

time 5, the BS using the proposed transfer learning algorithm transmits a standard VR image to the user while the BS using Q-learning transmits a cube image to the user. Therefore, at time slots 6 and 7, the BS using the proposed algorithm has no need to transmit VR images to the user while the BS using Q-learning needs to transmit a visible VR image to the user at time slot 7. This is due to the fact that the proposed transfer learning algorithm enables each BS to select the optimal image transmission format and, hence, the user can rotate the VR image received at time slot 5 and directly use the rotated VR images at time slots 6 and 7.

V. CONCLUSION

In this paper, we have developed a novel VR image transmission scheme that jointly consider various image formats and image rotation for optimizing the successful transmission probability of all VR users. We have formulated the problem as an optimization problem. To solve this problem, we have developed a novel transfer learning algorithm based on the liquid state machine. The proposed LSM-based transfer learning algorithm enables each BS adapts its image transmission scheme based on the users' image requests so as to maximize the users' successful transmission probability. Moreover, the proposed transfer learning algorithm can transfer the already learned successful transmission into the new successful transmission that must be learned as the users' VR image requests change. Simulation results have shown that the proposed transfer learning algorithm yields significant performance gains in terms of successful transmission probability of all VR users compared to Q-learning.

REFERENCES

- [1] E. Baştug, M. Bennis, M. Médard, and M. Debbah, "Towards interconnected virtual reality: Opportunities, challenges and enablers," *IEEE Communications Magazine*, vol. 55, no. 6, pp. 110–117, June 2017.
- [2] David P., "Facebook engineering," <https://www.facebook.com/Engineering/videos/10153781047207200/>.
- [3] F. Qian, L. Ji, B. Han, and V. Gopalakrishnan, "Optimizing 360 video delivery over cellular networks," in *Proc. of All Things Cellular (ATC) Workshop on Operations, Applications and Challenges*, New York, USA, 2016, Oct.
- [4] A. Rovira and M. Slater, "Reinforcement learning as a tool to make people move to a specific location in immersive virtual reality," *International Journal of Human-Computer Studies*, vol. 98, pp. 89–94, Feb. 2017.
- [5] O. Abari, D. Bharadia, A. Duffield, and D. Katabi, "Cutting the cord in virtual reality," in *Proc. of the ACM Workshop on Hot Topics in Networks*, Atlanta, GA, USA, Nov. 2016.
- [6] M. Chen, W. Saad, and C. Yin, "Virtual reality over wireless networks: Quality-of-service model and learning-based resource management," *available online: arxiv.org/abs/1703.04209*, Mar. 2017.
- [7] A. Taleb Zadeh Kasgari, W. Saad, and M. Debbah, "Human-in-the-loop wireless communications: Machine learning and brain-aware resource management," *arXiv preprint arXiv:1804.00209*, March 2018.
- [8] S. J. Pan and Q. Yang, "A survey on transfer learning," *IEEE Transactions on Knowledge and Data Engineering*, vol. 22, no. 10, pp. 1345–1359, Oct 2010.
- [9] M. Chen, U. Challita, W. Saad, C. Yin, and M. Debbah, "Machine learning for wireless networks with artificial intelligence: A tutorial on neural networks," *available online: arxiv.org/abs/1710.02913*, Oct. 2017.
- [10] I. Szita, V. Gyenes, and A. Lörincz, "Reinforcement learning with echo state networks," *Lecture Notes in Computer Science*, vol. 4131, pp. 830–839, 2006.
- [11] M. Bennis and D. Niyato, "A Q-learning based approach to interference avoidance in self-organized femtocell networks," in *Proc. of IEEE Global Commun. Conference (GLOBECOM) Workshop on Femtocell Networks*, Miami, FL, USA, Dec. 2010.